Design and Implementation of a Long-Range RFID Reader for Passive Transponders

Iker Mayordomo, Roc Berenguer, *Member, IEEE*, Andrés García-Alonso, *Member, IEEE*, Iñaki Fernández, and Íñigo Gutiérrez, *Member, IEEE*

***Abstract*—This paper presents a long-range RF identification (RFID) reader that has proven to work at up to 5 m with 2-W effective radiated power transmit power at 868 MHz. For the validation, a phase-shift keying backscatter modulator has been implemented, thus complementing the reader to form a complete passive RFID system focused on backscattering communication. The system has been first analyzed by means of a simulation tool, and as a result, reader design considerations are derived. Guidelines for the design of the backscatter modulator are also put forward. The reader and modulator have been fabricated and two measurement setups have been built to validate the reader performance. First, the system has been tested without antennas; −61.6-dBm reader sensitivity with only 11° phase difference has been measured. Finally, both the reader and modulator have been complemented with their respective antennas and the system has been evaluated in a real scenario. Reflections and interferences are demonstrated to degrade reader performance; nevertheless read ranges up to 8.1 m have been measured.**

***Index Terms*—Backscattering, reader, RF identification (RFID), ultra high frequency (UHF).**

I. Introduction

ONE OF the parameters that defines the performance of a passive RF identification (RFID) system is the read range. This is the maximum distance at which the power received by the transponder is strong enough to work properly, but also the maximum distance at which the backscattered power received by the reader is strong enough to be detected and properly demodulated. Since tag sensitivity today is much lower than reader sensitivity, most authors regard only the former as the condition to be fulfilled when working out the read range [1]–[3]. Under these premises, current short read ranges are caused by a low tag sensitivity and that is the reason why most efforts are currently focused on tag optimization.

As a result, tags achieving long read ranges have already appeared, 11 m at 868 MHz [4], 10 m at 950 MHz [5], and 12 m at 2.45 GHz [2]. In this new situation, the assumption typically made by authors is not entirely accurate. For long read ranges, new reader design constraints become apparent. Therefore, it becomes necessary to conduct an in-depth study on how reader-related parameters affect and/or limit the overall system performance. Moreover, proper long-range readers must be designed to take advantage of the improvements achieved in passive RFID tags, and thus, optimize the system read range, which definitely is one of the main objectives for the RFID research community.

This paper describes the design, implementation, and validation process of a long-range RFID reader working at 868 MHz. This paper is organized as follows. Section II describes the reader architecture; guidelines for the design of a phase-shift keying (PSK) backscatter modulator are also put forward. In Section III, the implemented modulator, as well as the measurement setups, are presented. Sections IV and V discuss the obtained results for both scenarios. Finally, a summary and conclusions are provided in Section VI.

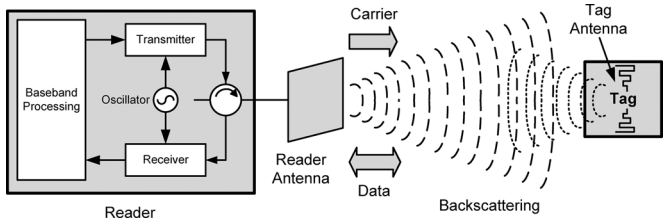

Fig. 1. Basic passive RFID system.

II. System Architecture

Passive transponders do not have their own power supply and, therefore, all the power required for their proper operation is drawn from the electromagnetic field transmitted by the reader. Reader-to-tag communication is done by means of an amplitude-shift keying (ASK) modulated carrier. Tag-to-reader communication is done by means of backscatter modulation. From the energy reaching the tag, a portion is used to supply tag circuits, the rest is backscattered. While the reader transmits an unmodulated carrier, the reflection coefficient of the transponder antenna is switched between two states in accordance with the data signal. Depending on whether either the resistance or reactance is varied, the backscattered carrier is modulated with ASK or PSK, respectively [6]. A basic passive RFID system is shown in Fig. 1.

Manuscript received May 23, 2008; revised January 15, 2009. First published March 31, 2009; current version published May 06, 2009. This work was supported by the Education, Universities and Research Department, Basque Country, and by the Spanish Ministry for Education and Science.

I. Mayordomo was with the Centro de Estudios e Investigaciones Técnicas (CEIT), Campus Tecnológico de la Universidad de Navarra (TECNUN), 20018 San Sebastián, Spain. He is now with the Fraunhofer Institut Integrierte Schaltungen (IIS), 91058 Erlangen, Germany (e-mail: imayordomo@ceit.es).

R. Berenguer, A. Garciá-Alonso, I. Fernández, and I. Gutiérrez are with the Centro de Estudios e Investigaciones Técnicas (CEIT), Campus Tecnológico de la Universidad de Navarra (TECNUN), 20018 San Sebastián, Spain (e-mail: rberenguer@ceit.es; angalonso@ceit.es; ifernandez@ceit.es; ingutierrez@ceit.es).

Digital Object Identifier 10.1109/TMTT.2009.2017291

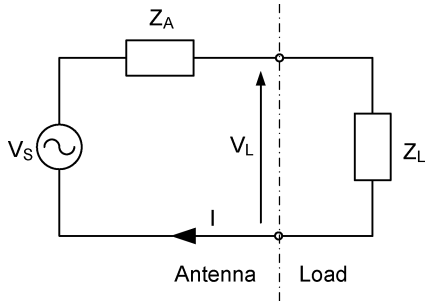

Fig. 2. Transponder equivalent circuit.

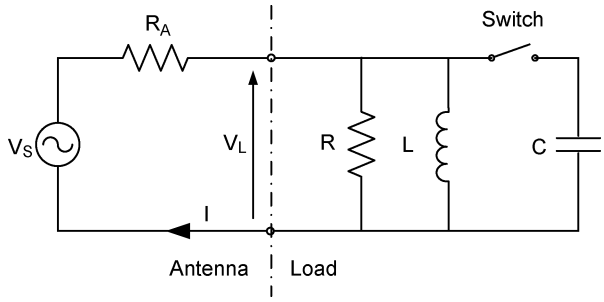

Fig. 3. PSK backscatter modulator equivalent circuit.

A. PSK Backscatter Modulator

The tag can be represented by its equivalent circuit, which is shown in Fig. 2. When the electromagnetic field coming from the reader is received, a voltage V_S is induced in the tag antenna, causing a current I through both the antenna impedance Z_A and the load impedance Z_L.

From the power reaching the antenna, only part is supplied to the load. This power reaching the load is proportional to the impedance mismatch factor q, which is defined as the relationship between the power that is supplied to the load and the maximum power that could be transferred [7]. Thus, the power that is transferred from the antenna to the load can be expressed as follows:

$$P_L = qP_{AV} = \frac{4R_A R_L}{|Z_A + Z_L|^2} P_{AV} \tag{1}$$

where P_{AV} is considered the maximum power available at the tag antenna and R_A and R_L are the antenna and load resistances, respectively.

As it can be seen in Fig. 2, the current I, which has been caused by the induced voltage V_S, also flows through the antenna resistance R_A. Thus, a power P_{BS} is caused in the antenna resistance [6]. This power is emitted, i.e., reflected back, by the tag antenna and can be worked out as follows:

$$P_{BS} = I^2 R_A = P_{AV} \frac{4R_A^2}{|Z_A + Z_L|^2}. \tag{2}$$

It is clear now that, modifying Z_L, the power reflected back by the tag antenna is altered. However, if the imaginary part of the load impedance Z_L is varied, not only variations in the amplitude, but also in the phase of the backscattered signal can be achieved.

As a conclusion, it can be stated that modulation of the input impedance of the tag results in amplitude and/or phase modulation of the backscattered signal, which is the basis for passive RFID systems. PSK modulation ensures a higher transfer of power from the antenna to the load. Furthermore, it allows this power to be constant during modulation [3], [4]. These are the main reasons why PSK backscatter modulation has been chosen for the system presented in this research.

PSK modulation works by modulating the tag input reactance. Thus, the phase of the current flowing through the antenna radiation resistance is modified, which makes the phase of the backscattered signal also vary. The model presented in Fig. 2 has been further developed, resulting in the model shown in Fig. 3.

The antenna, represented by the voltage source V_S and the resistance R_A, has been considered only resistive, with R_A equal to R to be close to the matching condition. Taking into account that the backscattered signal is proportional to the voltage on the radiation resistance V_{BS}, the phase of the backscattered signal reads

$$\theta = \arctan\left(\frac{\Im\{V_{BS}\}}{\Re\{V_{BS}\}}\right) = -\arctan\left(\frac{X_L}{R_A + R_L}\right) \tag{3}$$

where $R_L = \Re\{Z_L\}$ and $X_L = \Im\{Z_L\}$.

Thus, the phase of the backscattered signal results in

$$\theta = -\arctan\left(\frac{R_A X}{R_A^2 + 2X^2}\right). \tag{4}$$

Now, it is also interesting to work out which is the backscattered power and the power transferred to the load in case of PSK modulation. Applying (1) and (2) to the model represented in Fig. 3, expressions for both are obtained, respectively, as follows:

$$P_{BS} = P_{AV} \frac{4\left(R_A^2 + X^2\right)}{R_A^2 + 4X^2} \tag{5}$$

$$P_L = P_{AV} \frac{4X^2}{R_A^2 + 4X^2}. \tag{6}$$

A switch has also been included that, according to the data signal, makes the reactance X change between two different values X_{ON} and X_{OFF}. These are defined by

$$X_{\mathrm{ON}} = \frac{-j\omega L}{\omega^2 LC - 1} \tag{7}$$

$$X_{\mathrm{OFF}} = j\omega L. \tag{8}$$

These changes in the reactance make the reader signal be backscattered with two different phases, which are defined by (4).

In order to make both the backscattered power and the power transferred to the load remain constant, X must be modulated symmetrical to real part, which involves θ being also symmetrical. That is the reason why an inductance and a capacitance have been included. The inductances move the states towards

the positive part of the Smith chart ($X_{\mathrm{OFF}} > 0$) and the capacitances, on the other hand, do it to the negative part ($X_{\mathrm{ON}} < 0$).

Developing (4) and keeping the condition that makes the backscattered power remain constant, the following expressions are obtained:

$$\theta/2 = -\arctan \frac{R_A X_{\mathrm{ON}}}{R_A^2 + 2X_{\mathrm{ON}}^2} \tag{9}$$

$$-\theta/2 = -\arctan \frac{R_A X_{\mathrm{OFF}}}{R_A^2 + 2X_{\mathrm{OFF}}^2} \tag{10}$$

where θ represents the phase difference.

Once X_{ON} and X_{OFF} are obtained, the inductance L and the capacitance C can be easily worked out by means of (11) and (12) as follows:

$$L = \frac{X_{\mathrm{OFF}}}{\omega} \tag{11}$$

$$C = \frac{X_{\mathrm{ON}} - \omega L}{\omega^2 L X_{\mathrm{ON}}}. \tag{12}$$

As a result, a set of equations, that allows the tag model be designed to cause a predefined phase difference in the backscattered signal, has been defined. By means of this model, the tag-to-reader PSK backscattering communication have been included in the global design. Nevertheless, it must be reminded that this is a simplified model focused on backscattering communication. In most practical applications, RFID tags are designed to feature the lowest power consumption and highest efficiency, which may not match the previous guidelines.

B. Channel

In the propagation channel, free-space losses (FSLs) are considered. It must be taken into account that the transmitted signal crosses the propagation channel twice. Thus, the total FSLs during backscattering communication are given by (13) as follows:

$$FSL = \left(\frac{\lambda}{4\pi r}\right)^4 \tag{13}$$

where λ is the signal wavelength and r is the distance between the reader and the tag.

Since the phase in the reflected wave varies along time and distance, a phase shift has also been added to the channel model. This phase shift has no effect on PSK modulation since both phase states suffer the same shift. However, as will be explained later, depending on this phase shift, detection gaps can occur and quadrature downconversion is required in order to avoid them.

Finally, some polarization considerations must be taken into account. In most applications, the tag will appear always in an arbitrary position in the field of the reader antenna. Considering that, for size reasons, tag antennas are usually linear, the only way to guarantee the communication is by means of a circular antenna in the reader. Therefore, a 3-dB loss due to polarization mismatch must be considered, but the tag orientation problem is overcome [8].

C. Reader

Fig. 4 illustrates the block diagram of the designed reader, including the main parameters for every part in the design. As in most passive RFID readers, it is based on a direct conversion receiver [9]–[11], which reduces the complexity and number of components. The same local oscillator is used for both transmission and reception, image frequency problems are also avoided. However, as it will be explained in this section, there are several constraints inherited from the use of this architecture.

One of the main challenges that must be overcome is the transmission leakage into the receiver chain [12]. Passive RFID readers transmit a continuous wave and receive the backscattered data at the same time and at the same frequency. For that reason, the backscattered signal is masked by the transmission leakage reaching the receiver chain through the circulator. As a result, a very high dynamic range is required so that the receiver RF stage does not get saturated.

In the presented architecture, the power amplifier (PA) is able to transmit up to 2 W (33 dBm), amplifying the signal generated by the local oscillator and previously amplified by the driver. In this case, the signal reaches the receiver through the circulator, suffering a 33-dB attenuation. Considering a reader sensitivity of around -70 dBm [10], a 70-dB dynamic range would be required. Thus, the input 1-dB compression point (IP1 dB) and the input third-order intermodulation intercept point (IIP3) of both the low-noise amplifier (LNA) and the mixer are critical so that they do not get saturated and do not insert much distortion, which is not an easy task with circulator isolations around 30 dB. Some authors recommend that the LNA is not included to avoid this saturation [10], [13] at the cost of degrading the noise figure.

Although two antennas could be used simultaneously to provide higher isolation and reduce this transmission leakage, most commercial RFID readers use a single antenna with a circulator for its lower price and smaller size [10], [13]. It must be taken into account that the reader size is mainly imposed by the reader antenna.

Another design constraint of this architecture is that, due to the fact that the backscattered signal is masked by the transmission leakage and, probably, by strong reflections, coherent detection is not realizable [14]. This forces the reader to include an in-phase/quadrature (I/Q) demodulator in order to avoid detection gaps due to the phase shift introduced by the channel. Thus, when one path is at minimum sensitivity, the other is at maximum and the communication is always guaranteed [10].

DC offsets also appear due to self-mixing or due to strong reflections reaching the reader antenna. These offsets can be eliminated by placing an ac coupling stage as the first element in the baseband chain [9], as shown in Fig. 4. This avoids baseband stage from getting saturated [10] and the masked data can be recovered. A variable gain amplifier (VGA) has been included, providing the reader with a 40-dB baseband gain range. This allows the system operation for several distances. The antialiasing filter and the analog-to-digital converter (ADC) are designed to be able to work up to 1.5-MHz baseband bandwidth.

Finally, it was found out that during reader-to-tag communication, the baseband stage got completely saturated. The reason why this occurs is that the ac coupling stage is able to prevent dc offsets from getting the baseband amplifiers, but cannot do the same for modulated signals. Furthermore, it is required to set an initial condition for I and Q signals, as recommended by

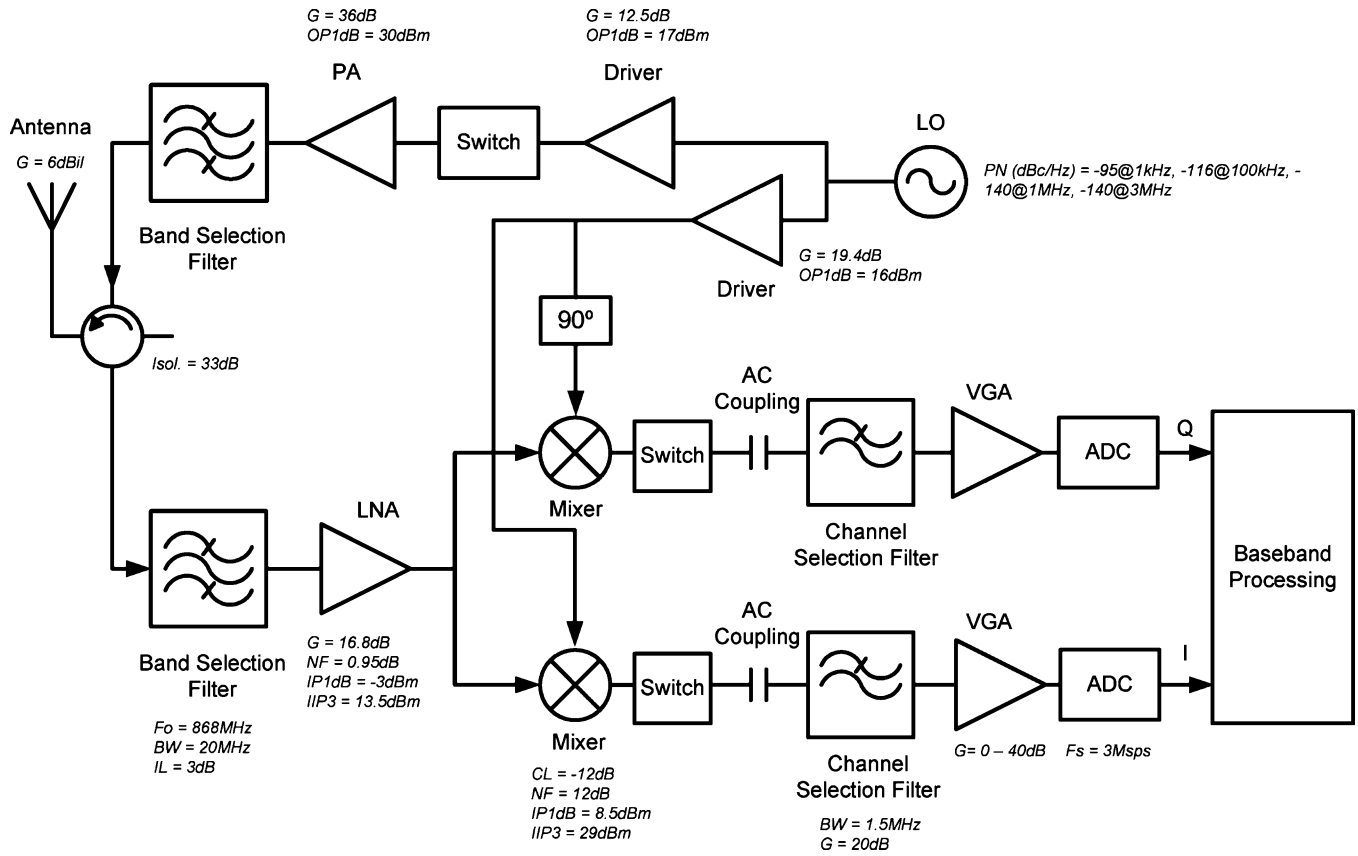

Fig. 4. Reader architecture. The designed reader architecture is based on a direct conversion receiver.

[10]. As a result, it is necessary to include a switch that disconnects the baseband stage during reader-to-tag communication, as shown in Fig. 4.

D. Demodulation

In order to work out the system bit error rate (BER), data must be demodulated. Baseband I and Q signals are given by (14) and (15), respectively, as follows:

$$i(t) = \sum_{m=0}^{\infty} ARect(t)\cos\left(\theta_m + \beta + \phi(t)\right) + n(t) \quad (14)$$

$$q(t) = \sum_{m=0}^{\infty} ARect(t)\sin\left(\theta_m + \beta + \phi(t)\right) + n(t) \quad (15)$$

where $\theta_m \in \{-\theta/2, \theta/2\}$ and $\phi(t)$ and $n(t)$ represent the phase noise and the noise floor at the baseband processing input, respectively. β is the variable that represents the phase shift that depends on both the channel phase shift and the oscillator phase. Due to this unknown β, quadrature downconversion is required, as already explained in Section II-C. $Rect(t)$ is given by (16) as follows:

$$Rect(t) = rect\left(\frac{t - T/4 - mT/2}{T/2}\right). \quad (16)$$

It must be taken into account that dc offsets have been eliminated by the ac coupling stage. As a result, the input of the demodulation block is a square signal without dc component whose amplitude depends on the backscattered power reaching the reader antenna and the receiver gain, which are represented by A, as well as on the phase components θ_m and β. This signal has an added noise, above all, due to the oscillator phase noise, the channel noise and the noise inserted by the receiver itself.

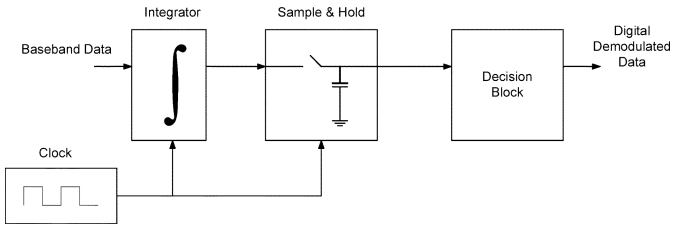

Fig. 5. Data demodulator. The demodulation is achieved by means of a noncoherent demodulator.

In this system, a noncoherent demodulator, shown in Fig. 5, has been implemented. The signal is integrated in the bit time interval and, by means of a sample and hold, the power level is kept. Last, a decision block obtains the demodulated data according to a predefined threshold. Both channels are processed independently and the one with best performance is chosen.

III. Simulation and Measurement Setups

In order to validate the designed reader, the system has not only been simulated, but also fabricated and measured. This section describes how these stages were carried out.

TABLE I
BACKSCATTER MODULATOR

	$Z_L(\Omega)$	Phase Difference (°)
Theoretical	$48.4 \pm j8.6$	10°
Measured	$49 + 9.8j$ $67 - 12.8j$	11°

A. Simulation Tool

A complete passive RFID system simulation environment has been developed in Agilent ADS, including the previously described models for the tag and the channel, as well as the completely designed reader architecture previously shown in Fig. 4. By means of this powerful simulation tool, the main design constraints that degrade reader performance can be analyzed, as previously reported by [15].

B. PSK Backscatter Modulator

Following the guidelines given in Section II-A, a PSK backscatter modulator, with a phase difference of 10°, has been designed. This value has been considered referring to [16], where 10° appears as a minimum or "worst case" phase difference. Firstly, the theoretical values are worked out, obtaining $L = 51.6$ nH and $C = 1.3$ pF as the values for the inductance and the capacitance, respectively. The backscatter modulator is then fabricated and its input impedance is measured by means of a network analyzer. Table I illustrates the input impedances for both modulation states, as well as the equivalent phase difference for the theoretical modulator and the fabricated modulator. The phase difference has been worked out by means of (4).

Finally, the tag model used in the simulation environment is redesigned to have the same values as the fabricated backscatter modulator. Thus, more accurate results will be achieved.

C. Measurement Setups

In order to validate the general system architecture and specifically the designed reader, a testing process has been planned. This has involved a series of measurements, which has been divided into the following two stages.

- *Measurements without antennas*. Firstly, the system operation has been evaluated without antennas. Thus, the efforts could be concentrated on analyzing the system performance without caring about propagation matters. As it will be explained in Section IV, the propagation channel has been replaced with a variable attenuator. As a result, the BER has been obtained according to channel attenuations, which have been later translated into distances by means of the Friis formula.
- *Measurements with antennas*. Once the system has been validated, it is time to test it under real conditions. This involves having both the backscatter modulator and the reader complemented with their respective antennas. As a result, propagation and matching troubles that did not occur during previous testing will become apparent.

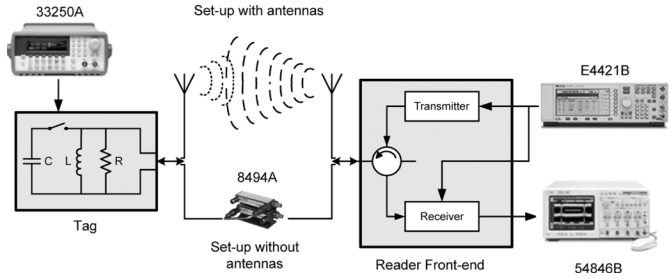

Fig. 6. Measurement setup scheme.

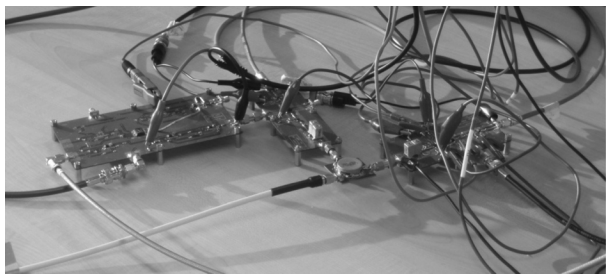

Fig. 7. Fabricated RFID reader.

The following sections describe the measurement setups that have been carried out in order to test the system, which are illustrated in Fig. 6, as well as the obtained results.

IV. MEASUREMENTS WITHOUT ANTENNAS

A. Setup

In this implementation, signal propagation will not occur through a real communication channel, but the tag and reader will be directly connected by means of a variable attenuator. The local oscillator in the reader has been implemented by means of a signal generator (Agilent E4421B). The baseband data coming from the reader front-end are digitalized by means of an oscilloscope (Agilent 54846B) to be later exported into ADS, where they are demodulated as explained in Section II-D. Finally, bits come into the backscatter modulator from a waveform generator (Agilent 33250A). This evaluation setup was first discussed in [17].

Fig. 7 shows the fabricated RFID reader, including the transmitter, receiver, baseband processing, and circulator.

B. Results

The simulation environment is configured to reproduce the same situation as the one previously illustrated in Fig. 6. Thus, the aim is not only to test the reader performance, but also to evaluate the developed simulation tool. The main system parameters are provided by Table II.

Fig. 8 shows the BER values that have been worked out for several channel attenuations. Considering a maximum BER of 10^{-3} [4], [18], the maximum channel attenuation allowed by this system would be 45.9 dB in case of the simulation and 44.3 dB for the measurement.

It can be noticed that the difference between both results is small. However, it would be more interesting for the purposes of this research that the results were translated into distances.

TABLE II
SYSTEM PARAMETERS

Parameter	Value
Phase difference	11°
Data rate	100Kbps
Phase noise	-95dBc/Hz@1kHz
Isolation	33dB
P_{reader}	27dBm

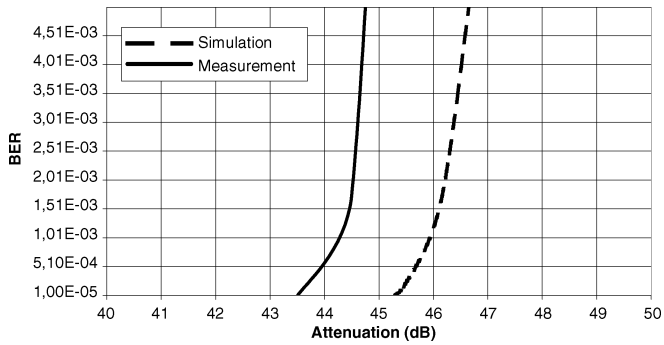

Fig. 8. BER versus channel attenuation.

Considering the Friis transmission formula, the relationship between channel attenuation and FSL is given by (17) as follows:

$$\text{att (dB)} = \frac{1}{2}(2\text{FSL} - G_{rc} - G_{rl} - G_t - k + p) \qquad (17)$$

where G_{rc} and G_{rl} represent the reader antenna circular and linear gains, respectively, G_t is the tag antenna gain, p is the polarization mismatch factor, and k is the portion of the power available at the tag antenna that is re-radiated according to (5).

Once equivalent FSL have been worked out, it is easy to translate them into equivalent distance by means of (18) as follows:

$$\text{FSL (dB)} = 20\log(r) + 20\log(f) - 147.56 \qquad (18)$$

where f represents the signal frequency (in hertz) and r is the distance (in meters) between the reader and tag.

Thus, by means of (17) and (18), previous results can be translated into distances, obtaining 12.7 and 11.3 m for simulation and measurement, respectively.

This difference between simulation and measurement can be due to small impedance mismatches in the block "PA–filter–circulator–attenuator" within the transmission chain. Any impedance variation can make the circulator isolation and/or the PA performance be altered, which can result in a overall performance decrease. Influence of circulator isolation on the system performance has been demonstrated by [15].

Finally, it is also possible to work out the reader sensitivity for both scenarios according to (19) as follows:

$$\text{Sens} = P_{\text{reader}} - 2Att + k \qquad (19)$$

Obtained reader sensitivities for both simulation and measurements are −64.8 and −61.6 dBm, respectively. It can be noticed that, as a result of the difference in the read range, the measured sensitivity differs 3.2 dB from the simulated one.

Fig. 9. Real scenario where the final measurements have taken place.

V. MEASUREMENTS WITH ANTENNAS

A. Setup

Although the previous setup is very useful in order to discard unwanted interferences, reflections, etc., and thus focus on the reader design, the obtained results cannot be considered as definite since they do not reflect what would be obtained in a real scenario. Therefore, in order to definitely validate the reader design and demonstrate its applicability for long-range RFID, the system must be tested in a completely real scenario. For that reason, this difference between simulation and measurement can be perfectly assumed.

Fig. 9 illustrates the environment where the measurements have taken place. As can be noticed, both the tag and reader are surrounded by all sort of objects, most of them metallic. It is worth pointing out that even both the floor and ceiling are composed of metallic materials. Thus, many unwanted effects can and will occur during measurements, degrading the system performance and limiting the read range that can be achieved.

As a consequence, both the reader and tag must be complemented with their respective antennas so that they are able to transmit and receive RF signals. For the tag, a dipole antenna tuned in the 865–868-MHz UHF band has been designed and fabricated. It features a meander dipole configuration in order to improve compactness and its resonant frequency has been estimated according to transmission line models. For simplicity, it has been implemented over a Flame Resistant-4 (FR4) substrate and i5ts gain has been estimated to be 2 dBil. For the reader, a circularly polarized commercial antenna with 7.8-dBic gain has been used.

B. Results

The main objective of this last stage is to check out which is the maximum read range at which the reader is capable of working when tested in a real scenario. In order to compare these results with the ones obtained without antennas, the main system parameters are the same as the ones previously provided by Table II.

Under these conditions, the system has proven itself to work at up to 8.1 m. However, the first thing to be noticed when

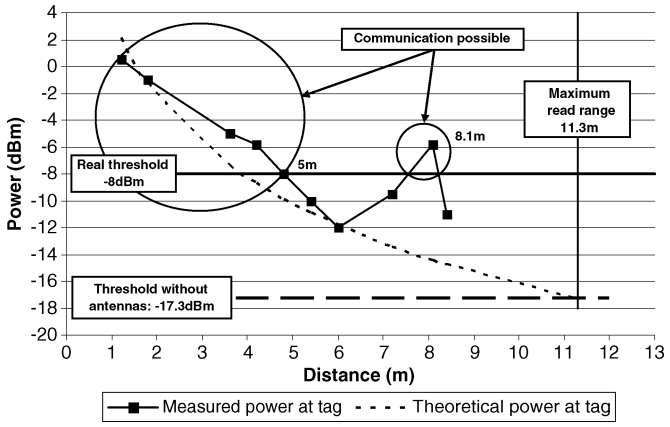

Fig. 10. System sensitivity in a real scenario.

testing the system in this real scenario has been the effect that reflections have on the system performance. To be precise, some zones where the communication was unachievable became apparent, even at shorter read ranges than zones where the communication was indeed possible.

As a result, it was considered necessary to verify how much power was reaching these zones so that the reason why this was happening could be understood. Therefore, the modulator was directly connected to the network analyzer so that the power reaching different zones of the laboratory could be measured. It was then verified that a minimum power of -8 dBm at the tag antenna was required for the system to work properly. This value differs from those of the simulation and the scenario without antennas, which are -18.9 and -17.3 dBm, respectively, according to (20) as follows:

$$P_{\text{tag}} = P_{\text{reader}} + G_{rl} - att + G_t. \tag{20}$$

The values of these measurements, as well as the read ranges at which the system worked, are shown in Fig. 10. The theoretical power that should reach the tag, according to (20), has also been included. Finally, the power threshold for both measurements, with and without antennas, has been drawn.

It can be observed that the system works perfectly up to 5 m. From 5 to 8 m, the power reaching the tag is then not enough and the communication is, therefore, not possible. Nevertheless, at 8.1 m, the power reaching the tag antenna turns out to be -6 dB and this is the maximum read range at which the system has been proven to be able to work. The 11.3-m limit, which is only achievable under ideal conditions, has also been included in the figure.

Due to reflections and as a result of constructive superposition, the power reaching the tag is at most points higher than the theoretical value. This phenomenon is commonly known as fading, and in this case, it could be seen as an advantage. However, this assumption is only accurate from the tag perspective and reader-to-tag communication point of view. From the reader's perspective, although there is more power to be backscattered, the effect of reflections and interferences will be much more degrading. This is not only because of reflected modulated signals that interfere with the main one, but also because of unmodulated reflected carriers that are added to the transmission leakage. The effect of transmission leakage on the reader performance was analyzed in [15]. As a result, it is not possible to precisely characterize the reader sensitivity in this real scenario and that is the reason why the power at the tag antenna has been used as reference.

VI. Conclusions

A complete reader architecture, which has definitely been demonstrated to be long range, has been presented in this paper. The reader has been fabricated and complemented with the implementation of a PSK backscatter modulator featuring a 11° phase difference, thus constituting a complete long-range RFID system focused on backscattering communication.

Two measurement setups have been built to carry out the reader validation. Firstly, the system has been tested without antennas. Maximum channel attenuations of 45.9 and 44.3 dB have been obtained for simulation and measurement, respectively. These values have been later translated into distances, obtaining 12.7- and 11.3-m read ranges. As already explained, this difference can be due to small impedance mismatches in the transmission chain that alter circulator isolation and/or PA performance. A reader sensitivity of -61.6 dBm has also been measured.

Last, the system performance has been checked with antennas. In this scenario, unwanted effects, such as reflections from metallic objects surrounding both the tag and reader, make the reader sensitivity be degraded, which consequently decreases the maximum read range that can be achieved. Nevertheless, the reader has proven to be able to work at up to 5 m in a completely adverse environment, as the presented laboratory is.

It must be pointed out these results have been obtained with only 11° phase difference in the PSK modulator, which actually is a worst case scenario. Phase difference can reach values up to 40° according to [16], which would greatly improve results according to the study previously conducted in [15].

Acknowledgment

The authors are grateful for the fruitful collaboration with the Mobile Radio Systems Group, Fraunhofer Institut Integrierte Schaltungen (IIS), Erlangen, Germany.

References

[1] K. V. S. Rao, P. V. Nikitin, and S. F. Lam, "Antenna design for UHF RFID tags: A review and a practical application," *IEEE Trans. Antennas Propag.*, vol. 53, no. 12, pp. 3870–3876, Dec. 2005.

[2] J.-P. Curty, N. Joehl, C. Dehollain, and M. J. Declercq, "Remotely powered addressable UHF RFID integrated system," *IEEE J. Solid-State Circuits*, vol. 40, no. 11, pp. 2193–2202, Nov. 2005.

[3] U. Karthaus and M. Fischer, "Fully integrated passive UHF RFID transponder IC with 16.7 μW minimum RF input power," *IEEE J. Solid-State Circuits*, vol. 38, no. 10, pp. 1602–1608, Oct. 2003.

[4] G. De Vita and G. Iannaccone, "Design criteria for the RF section of UHF and microwave passive RFID transponders," *IEEE Trans. Microw. Theory Tech.*, vol. 53, no. 9, pp. 2978–2990, Sep. 2005.

[5] T. Umeda, H. Yoshida, S. Sekine, Y. Fujita, T. Suzuki, and S. Otaka, "A 950 MHz rectifier circuit for sensor network tags with 10 m distance," *IEEE J. Solid-State Circuits*, vol. 41, no. 1, pp. 35–41, Jan. 2006.

[6] K. Finkenzeller, *RFID Handbook: Fundamentals and Applications in Contactless Smart Cards and Identification*, 2nd ed. New York: Wiley, 2003.

[7] K. Penttila, L. Sydanheimo, and M. Kivikoski, "Implementation of Tx/Rx isolation in an RFID reader," *Int. J. Radio Freq. Identification Technol. Appl.*, vol. 1, no. 1, pp. 74–89, 2006.
[8] Y. Tikhov, "Comments on 'Antenna design for UHF RFID tags: A review and a practical application'," *IEEE Trans. Antennas Propag.*, vol. 54, no. 6, pp. 1906–1907, Jun. 2006.
[9] P. B. Khannur, X. Chen, D. L. Yan, D. Shen, B. Zhao, M. K. Raja, Y. Wu, R. Sindunata, W. G. Yeoh, and R. Singh, "A universal UHF RFID reader IC in 0.18 μm CMOS technology," *IEEE J. Solid-State Circuits*, vol. 43, no. 5, pp. 1146–1155, May 2008.
[10] M. O'Neal, "UHF reader tutorial: A systems design perspective," in *IEEE MTT-S Int. Microw. Symp. Dig.*, San Francisco, CA, 2006.
[11] M. Reynolds and C. Weigand, "Design considerations for embedded software-defined RFID readers," *RF Design*, pp. 14–15, 2005.
[12] W. K. Kim, M. Q. Lee, J. H. Kim, H. S. Lim, J. W. Yu, B. J. Jang, and J. S. Park, "A passive circulator with high isolation using a directional coupler for RFID," in *IEEE MTT-S Int. Microw. Symp. Dig.*, 2006, pp. 1177–1180.
[13] "A compact RFID reader platform for UHF and microwave applications," WJ Commun. Inc., Hillsboro, OR, Tech. Rep., April 2004.
[14] Z. G. Fan, S. Qiao, J. T. Huangfu, and L. X. Ran, "Signal descriptions and formulations for long range UHF RFID readers," *Progr. Electromagn. Res.*, vol. 71, pp. 109–127, 2007.
[15] I. Mayordomo, A. Ubarretxena, D. Valderas, R. Berenguer, and I. Gutierrez, "Design and analysis of a complete RFID system in the UHF band focused on the backscattering communication and reader architecture," presented at the 3rd Eur. RFID Syst. Technol. Workshop, Duisburg, Germany, 2007.
[16] "Antenna matching for UHF—RFID yransponder ICs," ATMEL, San Jose, CA, Tech. Rep. ATA5590, 2005.
[17] I. Mayordomo, R. Berenguer, I. Fernandez, I. Gutierrez, W. Strauss, and J. Bernhard, "Simulation and measurement of a long-range passive RFID system focused on reader architecture and backscattering communication," presented at the 38th Eur. Microw. Conf., Amsterdam, The Netherlands, 2008.
[18] I. Kwon, Y. Eo, H. Bang, K. Choi, S. Jeon, S. Jung, D. Lee, and H. Lee, "A single-chip CMOS transceiver for UHF mobile RFID reader," *IEEE J. Solid-State Circuits*, vol. 43, no. 3, pp. 729–737, Mar. 2008.

Iker Mayordomo was born in Bilbao, Spain, in 1979. He received the M.S. degree in telecommunication engineering in 2003, and the Ph.D. degree from the Campus Tecnológico de la Universidad de Navarra (TECNUN), San Sebastian, Spain, in 2008.

From 2004 to 2008 he carried out research activities with both the Centro de Estudios e Investigaciones Técnicas (CEIT) and TECNUN. From 2005 to 2008, he was also a Lecturer with TECNUN. Since 2009, he has been with the Fraunhofer Institut Integrierte Schaltungen (IIS), Erlangen, Germany, where his research interests are focused on RFID systems.

Roc Berenguer (M'05) received the MSc. and Ph.D. degrees from the Engineering School, Tecnológico de la Universidad de Navarra (TECNUN), San Sebastian, Spain, in 1996 and 2000 respectively.

In 1999, he joined the Centro de Estudios e Investigaciones Técnicas (CEIT), as an Associate Researcher. He has collaborated in the design of several front-ends for wireless standards like WLAN, DVB-H, GALILEO, GPS, etc. He has also been as external consultant for Siemens, Hitachi, Seiko-Epson, etc. He is currently a Visiting Professor with the Illinois Institute of Technology, Chicago. He is also an Associate Professor of analog integrated circuits with TECNUN. His research interests include low-power analog circuit design and RFIC design for millimeter-wave circuits.

Andrés García-Alonso (M'08) was born in Bilbao, Spain, in 1964. He received the Ph.D. degree in 1993.

He is currently a Researcher with the Centro de Estudios e Investigaciones Técnicas (CEIT), and a member of the Engineering Faculty with the Tecnológico de la Universidad de Navarra (TECNUN), San Sebastian, Spain. For eight years, he was involved with thin films and silicon microsensors. From 1996 to 1997, he was with the Fraunhofer Institut für Integrierte Schaltungen (Fraunhofer IIS), Erlangen, Germany, where he was involved and continues to be involved with the design of analog integrated circuits for communication front ends. He has participated in in 12 industrial projects, and has managed five others. He has authored or coauthored 50 technical publications.

Iñaki Fernández was born on August 28, 1984. He received the Telecommunication Engineering degree from the Engineering School, Tecnológico de la Universidad de Navarra (TECNUN), San Sebastian, Spain, in 2007, and is currently working toward the Ph.D. degree at the Centro de Estudios e Investigaciones Técnicas (CEIT), San Sebastian, Spain.

His end of degree project has been developed in collaboration with CEIT working in RFID systems. His research is focused on digital cores of RFID readers.

Íñigo Gutiérrez (M'08) received the M.S. degree in industrial engineering and Ph.D. degree in electronics and communications engineering from the Tecnológico de la Universidad de Navarra (TECNUN), San Sebastian, Spain, in 1998 and 2004, respectively. His doctoral research concerned the design and characterization of integrated varactors for RF applications.

He is currently an Assistant Professor of basic electronics and general electronics with TECNUN. He has authored seven technical publications and has made eight contributions at international congresses. His current research interest includes RFID sensors.